


mTOR activation due to APPL1 deficiency exacerbates hyperalgesia via Rab5/Akt and AMPK signaling pathway in streptozocin-induced diabetic rats

Molecular Pain
Volume 15: 1–18
© The Author(s) 2019
Article reuse guidelines:
sagepub.com/journals-permissions
DOI: 10.1177/1744806919880643
journals.sagepub.com/home/mpx


Wan-You He¹, Bin Zhang¹, Wei-Cheng Zhao¹, Jian He¹,
Yunhua Wang¹, Lei Zhang¹, Qing-Ming Xiong¹, and
Han-Bing Wang¹ 

Abstract

Painful diabetic neuropathy is a common complication of diabetes mellitus with obscure underlying mechanisms. The adaptor protein APPL1 is critical in mediating the insulin sensitizing and insulin signaling. In neurons, APPL1 reportedly affects synaptic plasticity, while its role in the pathogenesis of painful diabetic neuropathy is masked. Our Western blotting revealed significantly decreased APPL1 expression in the dorsal horn in streptozocin-induced rats versus the control rats, coupled with concomitant mechanical and thermal hyperalgesia. Afterward, the determination of exact localization of APPL1 in spinal cord by immunofluorescent staining assay revealed highly expressed APPL1 in the lamina of spinal dorsal horn in control rats, with the overexpression in neurons, microglia, and underexpression in astrocytes. The APPL1 expression in laminae I and II was significantly downregulated in painful diabetic neuropathy rats. In addition, APPL1 deficiency or overexpression contributed to the increase or decrease of Map and Bassoon, respectively. The localization and immunoactivity of APPL1 and mammalian target of rapamycin (mTOR) were determined in spinal dorsal horn in painful diabetic neuropathy rats and control rats by immunohistochemistry, suggesting pronounced decrease in APPL1 expression in the superficial layer of the spinal cord in painful diabetic neuropathy rats, with p-mTOR expression markedly augmented. APPL1 knockdown by infection with lentiviral vector facilitated the activation of mTOR and abrogated mechanical withdrawal threshold values in painful diabetic neuropathy rats. Genetically overexpressed APPL1 significantly eliminated the activation of mTOR and resulted in the augmented mechanical withdrawal threshold values and thermal withdrawal latency values. Furthermore, the APPL1 levels affect phosphorylation of adenosine monophosphate-activated protein kinase (AMPK), and Akt, as well as the small GTPase, Rab5 expression in painful diabetic neuropathy rats. Our results uncovered a novel mechanism by which APPL1 deficiency facilitates the mTOR activation and thus exacerbates the hyperalgesia in streptozocin-induced diabetic rats, presumably via the regulation of Rab5/Akt and AMPK signaling pathway.

Keywords

Painful diabetic neuropathy, APPL1, mammalian target of rapamycin, hyperalgesia, Rab5

Date Received: 24 July 2018; revised: 6 August 2019; accepted: 4 September 2019

Introduction

Recent evidence indicates that diabetes mellitus (DM) has been a major public health hazard and rendered an enormous burden of socioeconomics, as evidenced by the data emanated from International Diabetes Federation that the world's 2015 diabetes health care costs amounted to \$673 billion and estimated to increase to \$802 billion in 2040.^{1,2} Painful diabetic neuropathy (PDN) is the most prevalent comorbidity of DM, with its prevalence markedly increasing in line with the

diabetic epidemic.³ PDN has a deleterious impact on life quality of patients owing to the painful burning, tingling, cramping, or shooting sensations.⁴ Thus far,

¹Department of Anesthesiology, The First People's Hospital of Foshan, Foshan, China

Corresponding Author:

Han-Bing Wang, Department of Anesthesiology, The First People's Hospital of Foshan, No. 81 North of Ling Nan Road, Foshan 528000, China.
Email: fswbhwang@126.com



however, the specific mechanisms contributing to PDN still remain elusive.⁵ In addition, due to the inadequacy and inefficiency of current therapeutic strategies available for PDN, less than 30% of patients could benefit from satisfactory pain relief.⁶ Precise molecular events underlying PDN await investigation and novel target candidates for the development of more effective pharmacological analgesics require identification.

The adaptor protein APPL1 (consisting of a plekstrin homology domain, phosphotyrosine-binding domain and leucine zipper motif) plays a crucial role in mediating the insulin-sensitizing effect of adiponectin in muscular and endothelial cells.^{7,8} Accumulating research works have validated that APPL1 exerts a direct effect on insulin signaling in cells.⁹ Genetic inhibition of APPL1 impaired insulin-stimulated Akt activation and membrane translocation of glucose transporter 4 (GLUT4) *in vitro* in the muscle cell and adipocytic cell lines.⁸ In addition, APPL1 overexpression in the liver potentiates insulin-mediated inhibition of hepatic glucose production and allays DM, while suppression of APPL1 expression gives rise to glucose intolerance.¹⁰ Emerging data have confirmed a multitude of functions of APPL1, e.g. convergence orchestration of multiple signaling pathways,¹¹ and facilitation of LKB1 translocation from the nucleus to the cytosol and phosphorylation of adenosine monophosphate-activated protein kinase (AMPK) in response to adiponectin stimulation as well as p38 mitogen-activated protein kinase (MAPK) activation by regulating the TAK1/MKK3/p38 MAPK cascade.^{12,13} APPL1 has been reported to elevate the insulin-mediated activity of Akt, as evidenced by the interaction with TRB3, an endogenous Akt inhibitor.¹⁰

Ample evidence suggested that neuronal synaptic plasticity is crucial to peripheral and central sensitization of neuropathic pain. Notably, APPL1 has been implicated in the PI3K-Akt pathway in response to growth factor signaling particularly in neurons, mediating the same pathway during dendritic spine and synapse formation and synaptic N-methyl-D-aspartate (NMDA)-receptor-dependent pro-survival signaling.^{14–16} Furthermore, APPL1 reportedly gates PI3K activation on the plasma membrane upon synaptic plasticity via its plekstrin homology domain and APPL1 knockdown (KD) in neurons impairs NMDA-receptor-dependent long-term potentiation. Therefore, there is a potential role of APPL1 in the onset and progression of hyperalgesia in PDN.

In this study, we assessed the variation of APPL1 expression and labeled its location in dorsal horn in streptozocin (STZ)-induced diabetic rats. The effect of APPL1 on synaptic plasticity was assessed thereafter. For investigation of the intracellular signaling involved, the localization and immunoactivity of APPL1 and mammalian target of rapamycin (mTOR) were

determined in the spinal dorsal horn in PDN rats and control rats by immunohistochemistry. To further explore the exact mechanism underpinning the regulation of mTOR and hyperalgesia by APPL1, genetic inhibition and overexpression of APPL1 in STZ-induced rats were employed by means of recombinant lentiviral vector system to test the relationship of APPL1 and AMPK and Akt. Ultimately, we interrogated the relationship of APPL1 and Rab5 for further investigation of the mechanism underlying the regulation of hyperalgesia by APPL1. Our experiment unraveled a novel mechanism by which APPL1 deficiency drives the mTOR activation contributing to hyperalgesia in STZ-induced diabetic rats, presumably via Rab5/Akt and AMPK signaling, and provided a potential target for the clinical regimen for PDN.

Materials and methods

Establishment of the rat model of DM

Healthy male Sprague–Dawley rats, weighing 180 to 220 g, were customized from Laboratory Animal Center of Guangdong Province and housed in the Experimental Animal Center for 3 to 5 days. The well-ventilated room was equipped with an air filtration system, with the room temperature (r/t) maintained at approximately 26°C and the humidity at 50% to 60%. The rats were allowed *ad libitum* access to food and water. All experimental procedures and protocols applied in this experiment were reviewed and approved by the Animal Care Committee of Sun Yat-Sen University and were performed in accordance with the guidelines on animal care from the National Institutes of Health and the ethical guidelines. The rats were fasted for 12 h prior to intraperitoneal injection of STZ (60 mg/kg; Sigma-Aldrich, USA) for diabetes induction, with those in the control group intraperitoneally injected with an equivalent volume of citric acid/sodium citrate buffer (pH = 4.5). Three days after STZ administration, the blood glucose levels were determined with Accu-Chek test strips (Roche Diagnostics, Indianapolis, IN, USA).

Intrathecal catheter implantation and drug administration

In order to ensure the precise injection of the drugs into the subarachnoid space of the lumbar enlargement, an intrathecal catheter was implanted as described.¹⁷ Cannulae were implanted into the rats under chloral hydrate (300 mg/kg) anesthesia. With a 1-cm midline incision in the atlanto-occipital membrane, polyethylene tubing (PE-10) was inserted into the subarachnoid space

and advanced rostrally for 2.5 cm at the level of the enlarged spinal cord lumbar segments. Thereafter, the catheter was attached to the dorsal paraspinal muscles and then subcutaneously tunneled to exit from the cervicodorsal region, where it was secured to the skin.

The rats were housed for four to five days for recovery prior to the administration of STZ or vehicle. The location of the PE-10 catheter was validated by the intrathecal administration of 15 μ L of 2% lidocaine, which induced paralysis of both hind extremities. Following intrathecal administration of the drugs (10 μ L), normal saline injection (15 mL) was maintained once daily for seven consecutive days. Rapamycin (5 μ g dissolved in 4% dimethyl sulfoxide (DMSO) in saline and sonicated prior to intrathecal injection), vehicle (4% DMSO of identical volume to rapamycin solution), APPL1 overexpression and APPL1-shRNA recombinant lentiviral vectors, or vacant lentiviral vectors were injected as appropriate.

Assessment of behavioral testing

All experiments were performed between 9:00 and 12:00 A. M. in a quiet environment. Briefly, the rats were positioned on the wire mesh cushion in individual compartments of metal and plexiglas for 15 to 20 min for acclimation. The mechanical withdrawal threshold (MWT) was assessed using von Frey filaments (Stoelting, Wood Dale, IL, USA) with 90° buckling forces between 2.0 and 15.0 g to stab the skin of third and fourth toes of right hind paws according to the up-down method.¹⁸ The weight on von Frey filaments was set as 2, 4, 6, 8, 10, or 15 g, with each stimulation duration of about 6 s at an interval of 1 min. Presence of quick withdrawal or licking of the paw in response to the stimulus was designated as a positive response. Mechanical allodynia was defined as a > 50% decrease in the MWT as compared to the baseline values.

The assessment of cold allodynia was conducted as previously described by immersing the tail in cold water (4°C).¹⁹ Briefly, each animal was lightly immobilized in a plastic holder, with its tail drooping for a proper application of cold water stimuli. After 5 cm of tail was immersed, the latency to an abrupt tail movement was measured with a cutoff time of 15 s. The tail immersion test was repeated five times at an interval of 5 min. In calculation of the average latency, the cutoff time was assigned to normal responses. The average latency was taken as a measure of the severity of cold allodynia (i.e. a shorter latency was interpreted as more severe allodynia). Cold sensitivity was measured with a hot/cold plate analgesimeter (UgoBasile, Milan, Italy). The rats were individually placed on the center of a cold plate maintained at 4°C in a transparent plexiglas cylinder for acclimation of 1 h. Escape behaviors were observed for 60 s and graded by the following scoring

system: 0 indicating no response; 1 indicating moderate effort to avoid cold, such as lifting a hind paw or walking backward and 2 indicating vigorous effort to escape cold, such as jumping. The scores recorded within a 60-s period were summed.

For thermal sensitivity testing, thermal withdrawal latency (TWL) in response to thermal hyperalgesia was assessed as previously reported.²⁰ The duration of the onset of the presence of withdrawal of hind paw from the infrared heating stimulus was recorded as TWL. Each hind paw was tested five times, with the first and last readings discarded. The mean response latency was calculated for statistical analysis.

Western blotting analysis

Under chloral hydrate (400 mg/kg) anesthesia, the enlarged spinal cord of rats were isolated and stored in liquid nitrogen until usage. The protein samples were extracted with their concentrations determined by bicinchoninic acid assay. Protein samples (30 μ g) were separated by sodium dodecyl sulfate-polyacrylamide gel electrophoresis and were transferred onto polyvinylidene fluoride membrane (300 mA, 2 h). Following the blockade with 5% non-fat milk in phosphate-buffered solution (PBS) solution for 1 h, the membranes were incubated with rabbit monoclonal anti-APPL1 antibody (1:1000; Santa Cruz, USA), rabbit polyclonal anti-mTOR antibody (1:1000; Santa Cruz, USA), rabbit monoclonal anti-phospho-mTOR antibody (p-mTOR, Ser2448, 1:1000; Cell Signaling Technology, USA), rabbit anti-Rab5 (1:1000; Cell Signaling Technology, USA), rabbit monoclonal anti-Akt (1:1000; Cell Signaling Technology, USA), rabbit monoclonal anti-p-Akt (T308, 1:1000; Cell Signaling Technology, USA), rabbit polyclonal anti-AMPK (Abcam, CA, UK), rabbit polyclonal anti-p-AMPK1 (1:1000, Ser485/Ser491; Affinity Biosciences, OH, USA), or anti-glyceraldehyde 3-phosphate dehydrogenase (GAPDH) antibody (1:1000; Hangzhou Goodhere Biotechnology Co. Ltd., China) overnight at 4°C. When rinsed thrice with PBS solution, the membranes were incubated with goat anti-rabbit IgG conjugated with the horseradish peroxidase (1:3000; Wuhan Boster Biological Technology Co. Ltd., China) for 45 min. With signal development performed with an enhanced chemiluminescent kit in ChemiDocTM MP Imaging System (Bio-Rad Co., USA), the mean density of the gray scale bands was quantified with QuantiScan 3.0 Demo gel image processing system (Bio-Rad, Inc., USA). To interpret the data of any minor variations in protein loading, the bands density was normalized with the corresponding GAPDH band density.

Recombinant lentiviral vector for APPL1 transgenic expression and KD

For local (dorsal horn) APPL1 overexpression, a commercial HIV-1-based recombinant lentiviral vector pCDH1-cytomegalovirus (CMV)-multiple cloning sites (MCS) EF-1a copGFP (SBI System Biosciences, Mountain View, CA, USA) was modified into vector pCDH1-CAG-attR1 CmRccdB attR2 EF-1a copGFP as previously reported. For gene transfection of spinal neuronal APPL1, we adopted dual promoter lentiviral vector to sustain activities of both APPL1 and EF-1a promoters in spinal dorsal horn neurons, with the enhanced green fluorescent protein as a reporter. To KD the APPL1 expression in the dorsal horn, an HIV-1-based recombinant Plvx-purolentiviral vector with a short hairpin RNA (shRNA) encoding APPL1 were employed. shRNA expression was driven by the human U6 promoter (pol III) cassette using the constitutively active human CMV promoter. Simultaneously, a vacant control lentiviral vector was employed as well. All pseudotypes of recombinant HIV vectors were packaged using a Lenti-XTM HT Packaging System (Clontech) with the human embryonic kidney 293 T cell line (293 T). The vector was purified using an iodixanol gradient and ultracentrifugation, followed by a buffer exchange procedure for further purification. The final virus in PBS solution had a titer of 1×10^8 viral particles/ml. The APPL1 transgenic expression, shRNA, or vacant lentiviral vector (1: 1: 1) was intrathecally injected into rats under anesthesia with sevoflurane in oxygen three weeks after STZ administration. For stable transgenic expression, the rats were allowed to recover for one week prior to biological detection. The efficacy of transgenic expression or shRNA KD of APPL1 was validated by qPCR. Total mRNA in the enlarged lumbar spinal cords were extracted with a homogenizing kit (Tel-Test, Friendswood, TX, USA), which isolated the RNA from DNA and protein using chloroform and was precipitated with isopropanol. Contaminated DNA was removed with Turbo DNA-free (Life Technologies, CA, USA) using a rigorous protocol and 5 μ g of purified RNA was reverse transcribed into cDNA (Invitrogen SuperScript III First-Strand Synthesis System). The resultant cDNA was quantified via qPCR using a SYBR Green method.

Immunocytochemistry

The rats were deeply anesthetized with an injection of chloral hydrate (400 mg/kg) and perfused with 4% paraformaldehyde for immunohistochemical assay. Enlarged lumbar spinal cords were isolated, post-fixed at 4°C for 4 h and were thereafter immersed in 30% (w/v) sucrose solution at 4°C for 24 h.

For single-labeling immunofluorescence assay, transverse spinal cord sections (at the thickness of 25 μ m) were incubated in a blocking solution (5% v/v normal goat serum) for 1 h at room temperature and incubated with the following primary antibodies: anti-Rab5 (rabbit monoclonal, 1:200 dilution; Santa Cruz Biotechnology), Map2 (rabbit monoclonal, 1:200, Abcam), and Bassoon (rabbit monoclonal, 1:200, Cell Signaling Technology) overnight at 4°C. After the sections with the primary antibodies were incubated, species-specific secondary antibodies were added for incubation of 4 h in buffer containing goat anti-rabbit IgG (1:200 dilution, Boster Biological Technology) and Cy3-conjugated goat anti-mouse IgG (1:200 dilution; Boster Biological Technology) at room temperature in the darkness. Thereafter, the slices were stained with 4',6-diamidino-2-phenylindole (1:5,000 dilutions). Finally, after having been rinsed with PBS, the sections were mounted onto clean glass slides, air-dried, and cover-slipped with a mixture of 0.05 M PBS containing 50% (v/v) glycerin and 2.5% (w/v) triethylenediamine.

For double-labeling immunofluorescence histochemistry, transverse spinal cord sections (at the thickness of 10 μ m) were incubated in a blocking solution (5% v/v normal goat serum) for 1 h at room temperature and incubated overnight at 4°C with the following primary antibodies: (1) a mixture of rabbit monoclonal anti-APPL1 (1:200 dilution; Santa Cruz Biotechnology) and mouse monoclonal anti-NeuN (1:500, Abcam), mouse monoclonal anti-gial fibrillary acidic protein (GFAP) (1:200, Cell Signaling Technology), mouse monoclonal anti-OX42 (1:100, Santa Cruz Biotechnology), mouse monoclonal anti-calcitonin gene-related peptide (CGRP) (1:100, Santa Cruz Biotechnology), biotinylated IB-4 (1:100, Santa Cruz Biotechnology), or mouse monoclonal anti-nuclear factor (NF)-200 and (2) a mixture of rabbit monoclonal anti-Rab5 (1:400, Cell Signaling Technology) and mouse monoclonal anti-NeuN (1:500, Abcam), mouse monoclonal anti-GFAP (1:200, Cell Signaling Technology), mouse monoclonal anti-OX42 (1:100, Santa Cruz Biotechnology), mouse monoclonal anti-CGRP (1:100, Santa Cruz Biotechnology).

The sections were then incubated with a mixture of Cy3-conjugated species-specific goat anti-rabbit IgG Cy3 (1:100, Wuhan Boster Biological Technology) and fluorescein isothiocyanate (FITC)-conjugated mouse FITC-labeled goat anti-mouse (1:100, Wuhan Boster Biological Technology) for 1 h at 37°C in dark.

The sections were observed under a confocal laser scanning microscope (FV-1000, Olympus, Tokyo, Japan). The images were captured and quantitatively analyzed with ImageJ software (National Institutes of Health (NIH), Bethesda, MD, USA). The spinal slices were directly stained with Cy3-conjugated and FITC-conjugated species-specific secondary antibodies as the

specificity controls. Multiple visual fields ($n=4$) in each experimental group were subjected to a threshold in order to eliminate all background and non-relevant pixels. The images were then quantified using the total pixel count above threshold, and the resulting data were imported into GraphPad Prism software (GraphPad Software, San Diego, CA, USA) for statistical analysis.

All cells with labeled or unlabeled nuclei were counted. Cell profiles were outlined and cell area was calculated with ImageJ software (NIH, Bethesda, MD, USA). To analyze the 10 groups of double-labeled sections from the enlarged lumbar spinal cords, sections from three rats (2 spinal cords/rat; 10–12 sections/spinal cord) were randomly chosen for each group. Single-labeled and double-labeled neurons were counted. Two independent pathologists blinded to the assignment and treatment scored the samples and the region of the spinal dorsal horn (Figure 1). The intensity of staining was scored as follows: 1 = negative positivity, 2 = modest positivity, 3 = moderate positivity, and 4 = intense positivity. The percentage of membranous and cytoplasmic staining in malignant cells was scored into four categories: 1: 0% to 25%; 2: 26% to 50%; 3: 51% to 75%; 4: 76% to 100%. The final scores were computed by the intensity score multiplied by the scores for the percentage counts. Any neuron with a score >6 was considered as positive neuron.

Statistical analysis

All statistical analyses were assessed with SPSS version 15.0 statistical software. The quantitative data are expressed as the means \pm SEM. In the case of eligibility of normality and homogeneity of variance assumptions, one-way analysis of variance was employed for comparisons among multiple groups, followed by comparison between two groups with the least significant difference (LSD) method (Fisher's LSD test), with the criterion for statistical significance set at $P < 0.05$.

Results

Significant downregulation of spinal APPL1 in rats with painful diabetic neuropathy

To explore the variations of APPL1 in progressive hyperalgesia, its protein expression in spinal cord in PDN rats was determined. Following a single intraperitoneal injection of STZ or control vehicle, the body weight, blood glucose, MWT, TWL, and cold withdrawal scores (CWS) in rats were monitored for four weeks. Along with elevated blood glucose levels, the tests with von Frey filaments revealed that the MWTs were significantly decreased as from the second week and reached the nadir at fourth week postinjection in the STZ-injected rats versus the control rats ($P < 0.05$; Figure 2(a)). The values of TWL

were significantly reduced in the third week and maintained till week 4 ($P < 0.05$; Figure 2(b)). The value of CWS was pronouncedly elevated in two to three weeks ($P < 0.05$; Figure 2(c)) and reversed to the baseline at fourth week, with insignificant statistical difference ($P > 0.05$; Figure 2(c)). All behavior tests indicated that the rats exhibited mechanical and thermal hyperalgesia in week 4. Western blotting assay indicated that the downregulation of APPL1 commenced at week 1 and was pronouncedly decreased until week 4 in PDN rats versus the control rats ($P < 0.05$; Figure 2(d)). These data revealed that APPL1 was significantly eliminated in STZ-induced diabetic rats and contributed to hyperalgesia.

Cellular localization of APPL1 in spinal cord in STZ-induced diabetic rats with PDN

Subsequently, we further determined the cellular localization of APPL1 by means of immunofluorescent staining assay in the spinal cord in control rats and PDN rats. In normal condition, APPL1 ($46\% \pm 7.3$) is abundantly expressed in spinal dorsal horn neurons, suggestive of the co-expression with NeuN, a specific marker for neural nuclei, and in the microglia ($83\% \pm 6.9$), indicative of co-expression with OX-42, a microglia marker, whereas the positivity of APPL1 ($13.7\% \pm 3.4$) in astrocytes was relatively weak, evidenced by co-localization of GFAP, a astrocyte marker (Figure 3(a) to (c)). In contrast, the APPL1 expression in spinal dorsal horn neurons, microglia, and astrocytes was pronouncedly downregulated, particularly in the lamina of spinal dorsal horn in the PDN rats versus the control rats (Figure 3(a) to (c)). In addition, we also noted that the astrocytes were significantly activated in PDN rats as compared to the control rats (Figure 3(b)). Moreover, to further address the localization of APPL1 in the lamina of the spinal dorsal horn, selective laminar markers were employed. The results of the immunofluorescent assay revealed that APPL1 was abundantly expressed in the surface layer of lamina I and relatively overexpressed in lamina II in the control rats, supported by the evidence of the co-expression with IB-4 and CGRP, respectively (Figure 3(d) and (e)). The APPL1 expression was significantly decreased in both the lamina I and lamina II in PDN rats compared with the control rats (Figure 3(d) and (e)). APPL1 was also co-expressed with NF200, a marker for myelinated A-fibers, suggesting the location of APPL1 in the lamina III-VI (Figure 3(f)), where its expression level was slightly decreased in PDN rats (Figure 3(f)). Consistent with the control group, no immunofluorescence was detected in the dorsal horn when the primary antibodies were omitted, pre-absorbed with an excess of the corresponding antigen, or replaced with normal IgG during the staining procedure (Figure 3(g)).

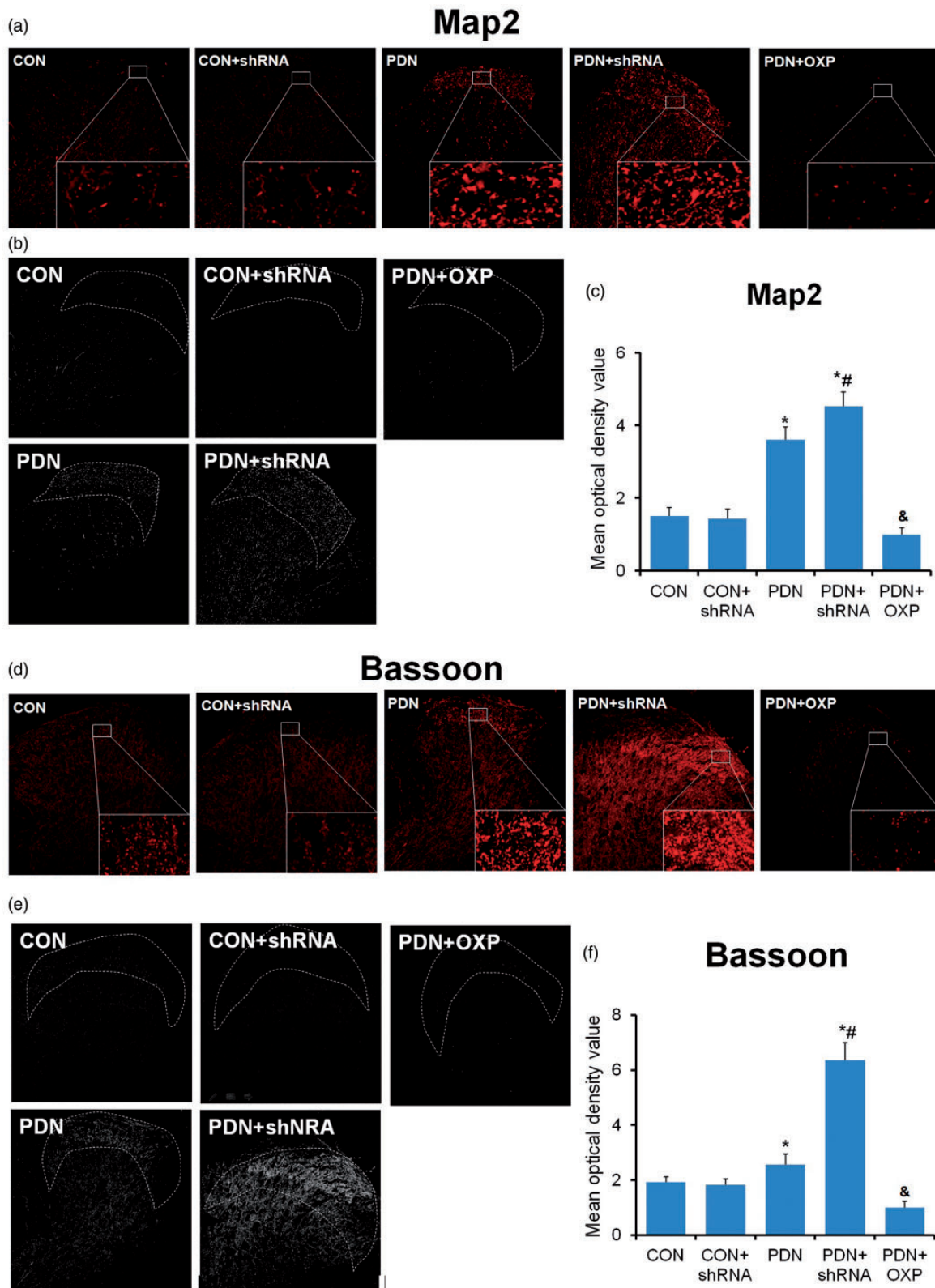


Figure 1. Effects of APPLI on the formation of dendritic spine and synapse in STZ-induced diabetic rats. (a) to (c) The immunofluorescent staining for Map2 in control rats, PDN rats, APPLI-deficient PDN rats, and APPLI-overexpressed PDN rats. (d) to (f) The immunofluorescent staining for Bassoon in control rats, PDN rats, APPLI-deficient PDN rats, and APPLI-overexpressed PDN rats. The abbreviations for the groups of normal control (CON), CON + shRNA recombinant lentiviral vector, painful diabetic neuropathy + vacant lentiviral vector (PDN), PDN + shRNA recombinant lentiviral vector and PDN + APPLI overexpression recombinant lentiviral vector are shown as CON, CON + shRNA, PDN, PDN + shRNA and PDN + OXP. (n = 20, *P < 0.05 vs. control group). Data are expressed as the means \pm SEM.

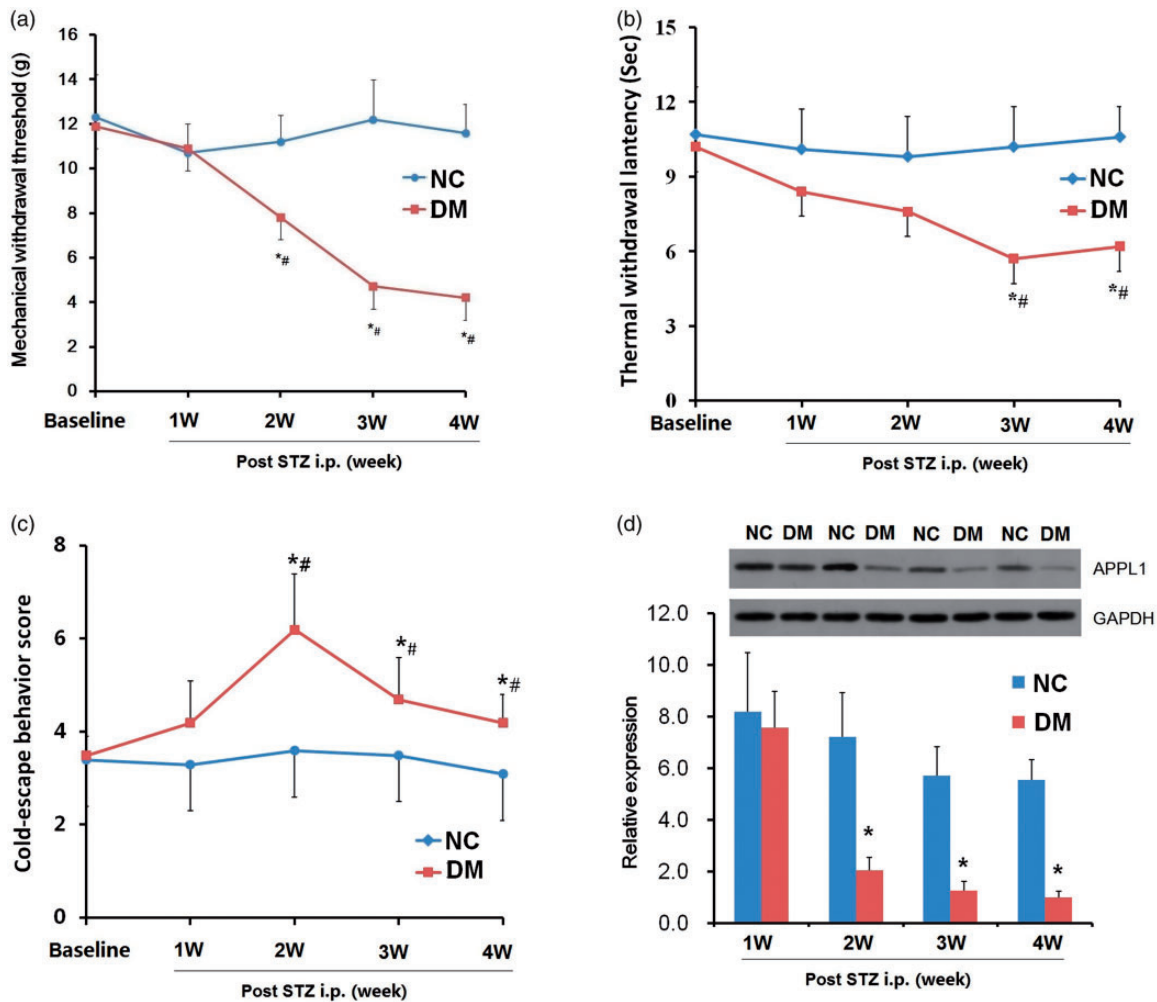


Figure 2. The alterations of MWT, TWL and CWS and APPL1 protein levels in STZ-induced diabetic rats. (a) The MWT variations in STZ-induced diabetic rats and control rats. (b) The TWL variations in STZ-induced diabetic rats and control rats. (c) The variations of cold pain hypersensitivity in STZ-induced diabetic rats and control rats. (d) The expression of APPL1 in STZ-induced diabetic rats and control rats. The abbreviations for the groups of normal control, diabetes are shown as NC and DM ($n = 6$ for behavioral tests, $n = 4$ for Western blotting assay, $*P < 0.05$ vs. NC group, $^{\#}P < 0.05$ vs. baseline). Data are expressed as the means \pm SEM.

The alterations of the formation of dendritic spine and synapse related to APPL1 in the spinal cord in STZ-treated diabetic rats

Dendritic dysgenesis on nociceptive sensory neurons and nociceptive synapse have been identified to play an evident role in neuropathic pain.^{21,22} APPL1 was mainly localized in the dendrites of neurons.²³ Hence, we assessed the changes in formation of dendritic spine and synapse under APPL1-deficient or overexpressed condition in the control and PDN rats. Both Map (a marker of dendritic spine) and Bassoon (a marker of synapse) were significantly upregulated in PDN rats versus control rats ($P < 0.05$; Figure 1), indicating the involvement of the formation of dendritic spine and synapse. KD of APPL1 further enhanced the formation of

dendritic spine and synapse in diabetic rats rather than normal control rats. In contrast, APPL1 overexpression significantly eliminated the formation of dendritic spine and synapse (Figure 1). All the findings suggested that APPL1 could alleviate the hyperalgesia of PDN rats probably via the negative regulation of formation of dendritic spine and synapse.

Co-expression of APPL1 with mTOR and negative regulation of its activity in the spinal dorsal horn in PDN rats

On the grounds that mTOR plays a crucial role in neuropathic pain, doubts remained as to whether the involvement of APPL1 in PDN rats was associated with mTOR. To decipher the relevance of APPL1 and

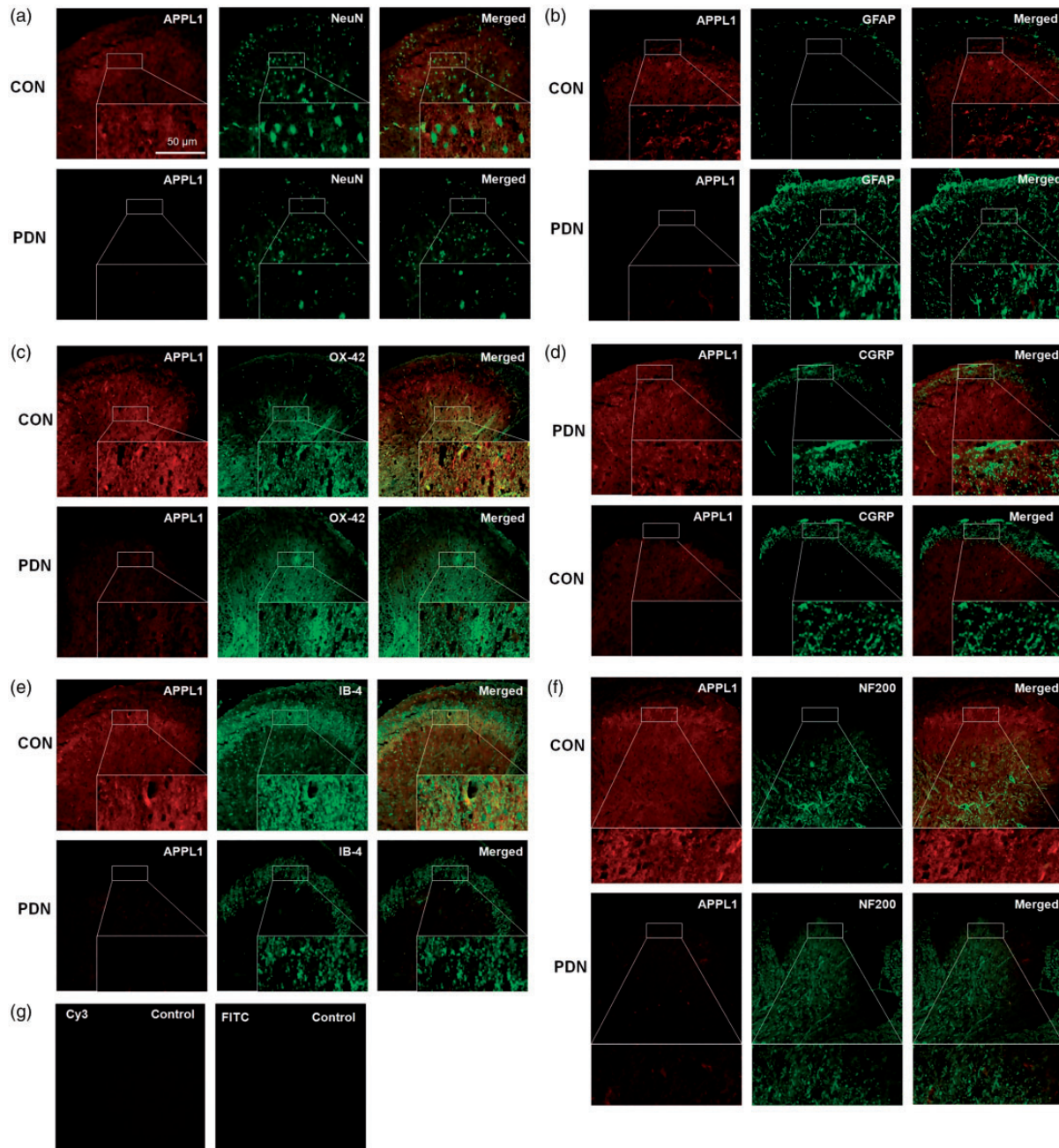


Figure 3. The localization and distribution of APPL1 in spinal cord in PDN rats. (a) to (f) Double labeling of APPL1 (red) with NeuN (green), GFAP (green), OX-42 (green), CGRP (green), IB-4 (green), and NF200 (green) in spinal dorsal horn in PDN rats, and CON rats. (g) The spinal slices were directly stained with Cy3-conjugated and FITC-conjugated species-specific secondary antibodies as the specificity controls. PDN: painful diabetic neuropathy; CON: normal control.

mTOR, the distinct localizations of APPL1 and p-mTOR in the spinal cord were determined by means of immunohistochemistry. The results unveiled that APPL1 was widely expressed in both the gray matter and the white matter of the lumbar spinal cord in the control rats, with the higher density of APPL1 and

p-mTOR signals located in the superficial layer of the spinal dorsal horn, laminae I and II, wherein the fundamental location in nociceptive transmission in the spinal cord was considered (Figure 4(a) and (b)). Of note, APPL1 expression was heavily co-expressed with p-mTOR in the superficial layer of the spinal cord in

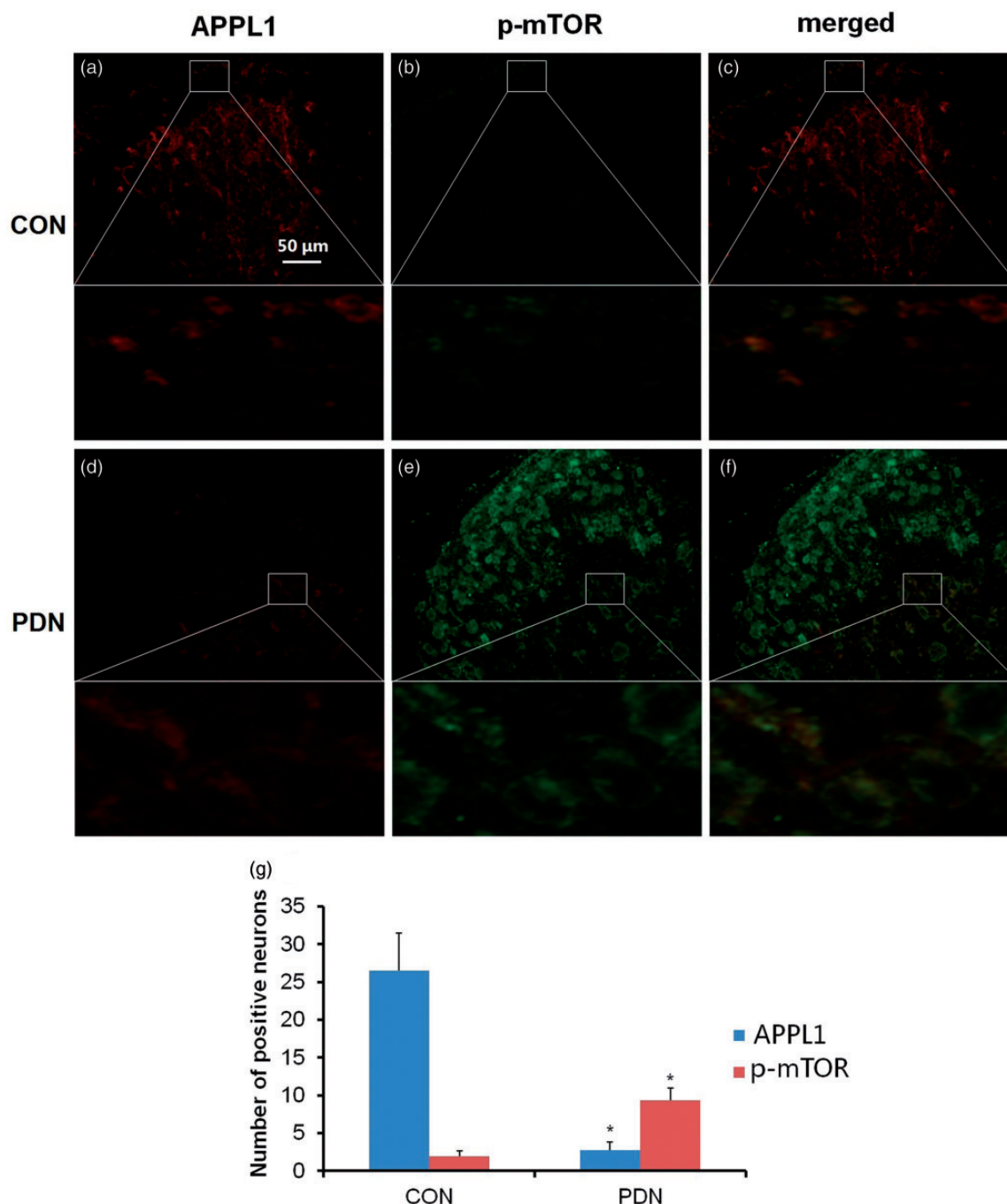


Figure 4. The double labeling of APPL1 (green) and p-mTOR (red) in control rats and PDN rats. The abbreviations for the groups of control, painful diabetic neuropathy (PDN) are shown as CON, PDN ($n = 20$, $*P < 0.05$ vs. control group). Data are expressed as the means \pm SEM.

normal control rats (Figure 4(c)). In contrast, the immunoreactivity of APPL1 was significantly dampened, accompanied by tremendous expression of p-mTOR in PDN rats versus the control rats ($P < 0.05$; Figure 4(d) to (g)). These data suggested that the APPL1 was mainly co-expressed and negatively regulated the mTOR activity in the spinal dorsal horn.

APPL1 KD evoked the mTOR activation and aggravated hyperalgesia in diabetic rats

To probe the functional role of the APPL1 in PDN and the exact effect on the modulation to mTOR in vivo, we employed a recombinant lentiviral vector system to genetically KD APPL1 expression. The efficacy of APPL1 KD

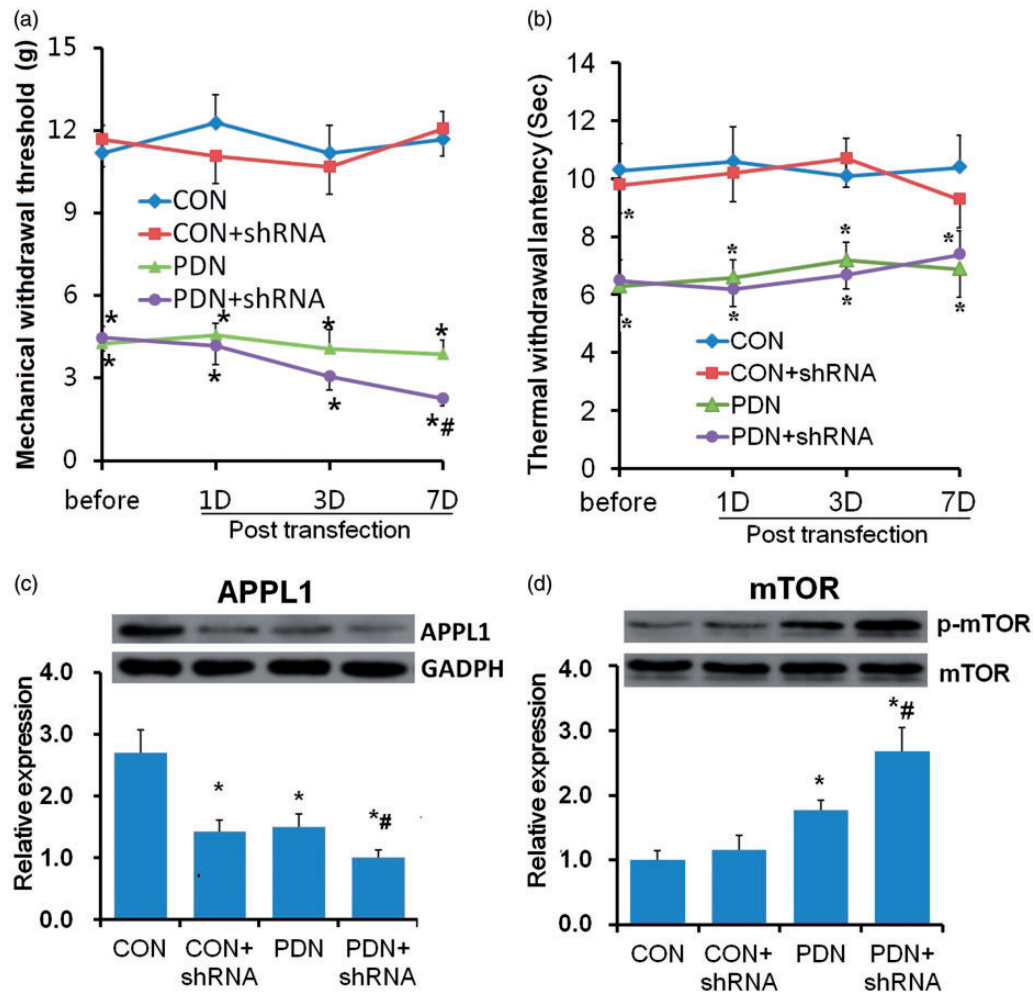


Figure 5. Effects of APPL1 genetic knockdown on the expression of p-mTOR and hypersensitivity in STZ-induced diabetic rats. (a) The MWT values in normal control rats, PDN rats, and PDN rats infected with shRNA encoding APPL1. (b) The TWL values in normal control rats, PDN rats, and PDN rats infected with shRNA encoding APPL1. (c) The protein expression of APPL1 in spinal dorsal horn in control rats, PDN rats, and PDN rats infected with shRNA encoding APPL1. (d) The expression of p-mTOR in spinal dorsal horn in control rats, PDN rats, and PDN rats with APPL1 knockdown. The abbreviations for the groups of normal control (CON), CON + shRNA encoding APPL1 (shRNA) painful diabetic neuropathy + vacant lentiviral vector (PDN) and PDN + shRNA are shown as CON, CON+shRNA, PDN and PDN+shRNA ($n = 6$ for behavioral tests, $n = 4$ for Western blotting assay, $*P < 0.05$ vs. CON group, $^{\#}P < 0.05$ vs. PDN). Data are expressed as the means \pm SEM.

was confirmed by the Western blotting analysis, which exhibited that the protein levels of APPL1 were conspicuously abrogated in normal control rats and PDN rats infected with shRNA specific to APPL1 versus the PDN rats (Figure 5(c)). The behavioral test results showed that the MWTs of the PDN rats treated with APPL1 shRNA vector were significantly decreased versus those treated with vacant lentiviral vector but there was no significant effect of APPL1 KD in normal rats. ($P < 0.05$; Figure 5 (a)), indicating the KD of APPL1 aggravated the hyperalgesia in PDN rats. However, the TWLs of the normal control rats and the PDN rats treated with APPL1 shRNA vector were not altered versus those treated with vacant lentiviral vector ($P > 0.05$; Figure 5(b)). In parallel with the results of Western blotting, the protein levels of p-

mTOR were further upregulated in PDN rats infected with lentiviral vector encoding shRNA specific to APPL1 versus PDN rats, and likewise, APPL1 KD had no marked effect on the levels of p-mTOR in normal rats ($P < 0.05$; Figure 5(d)), suggesting that APPL1 deficiency only produced an effect on promoting the mTOR activation in the spinal cord and exacerbated the mechanical hyperalgesia in PDN rats.

APPL1 overexpression impaired the mTOR activation and alleviated hyperalgesia in STZ-induced diabetic rats

To further corroborate the effects of transgenic expression of APPL1 on PDN, the rats were transfected with

APPL1 gene by means of the classical method of recombinant lentivirus transfection to overexpress the APPL1 level. The overexpression was validated by Western blotting analysis, which revealed that APPL1 expression was remarkably enriched in behavioral data at day 4 after intrathecal transfection with recombinant lentivirus vectors encoding APPL1 gene ($P < 0.05$; Figure 6(c)). MWTs and TWLs were remarkably elevated in PDN rats versus the control rats ($P < 0.05$; Figure 6(a) and (b)), suggesting the inhibitory effect of APPL1 overexpression on the

mechanical and thermal hyperalgesia in STZ-induced diabetic rats.

Moreover, Western blotting analysis demonstrated that the protein levels of p-mTOR was significantly attenuated in response to APPL1 overexpression in the spinal cord in diabetic rats ($P < 0.05$; Figure 6(d)), indicating the suppressive effect of APPL1 overexpression on mTOR activation. Furthermore, the mTOR inhibitor, rapamycin, was employed to explore the effect of mTOR in the regulation of hyperalgesia by APPL1 in PDN rats. Rapamycin markedly increased the MWTs and TWLs

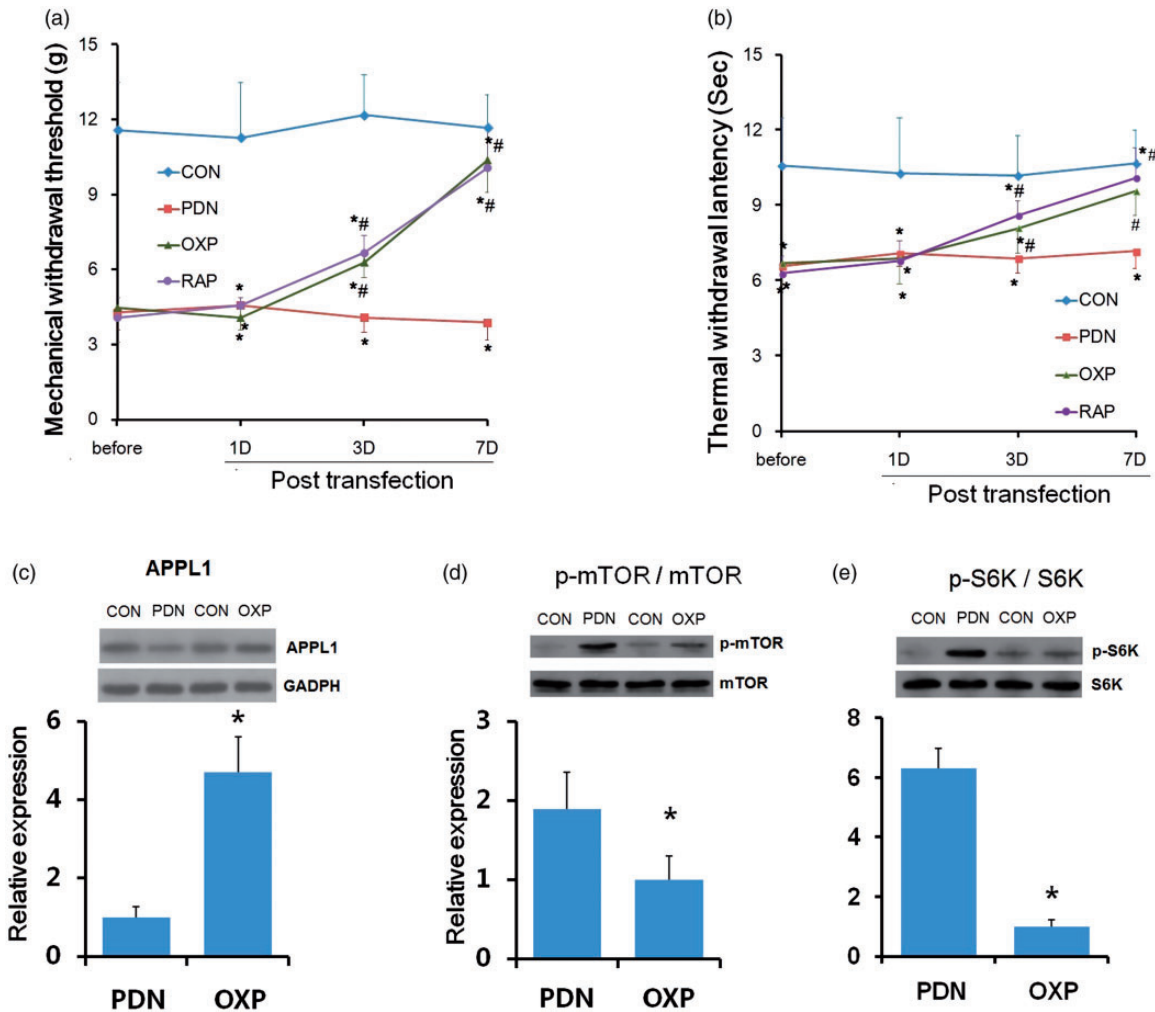


Figure 6. Effects of genetic overexpression of APPL1 on the expression of p-mTOR and hypersensitivity in STZ-induced diabetic rats. (a) The MWT values in control rats, PDN rats, PDN rats infected with APPL1 overexpression, and PDN rats treated with rapamycin (RAP). (b) The TWL values in control rats, PDN rats, PDN rats infected with APPL1 overexpression, and PDN rats treated with rapamycin. (c) The protein expression of APPL1 in spinal dorsal horn in control rats, PDN rats, and PDN rats with APPL1 overexpression. (d) The expression of p-mTOR in spinal dorsal horn in control rats, PDN rats, PDN rats with APPL1 overexpression, and PDN rats treated with rapamycin. (e) The expression of p-S6K in spinal dorsal horn in control rats, PDN rats, and PDN rats treated with rapamycin. The abbreviations for the groups of normal control, painful diabetic neuropathy (PDN) + vacant lentiviral vector, PDN + APPL1 genetic overexpression and PDN + rapamycin are shown as CON, PDN, OXP and RAP. ($n = 6$ for behavioral tests, $n = 4$ for Western blotting assay; $*P < 0.05$ vs. CON group, $^{#}P < 0.05$ vs. PDN group in Figure 6(a) and (b); $*P < 0.05$ vs. PDN group in Figure 6(c) to (e)). Data are expressed as the means \pm SEM.

in PDN rats versus the control rats ($P < 0.05$; Figure 6(a) and (b)). Indeed, the p-S6K expression was evidently inhibited by rapamycin treatment ($P < 0.05$; Figure 6 (e)). Taken together, these results indicated a specific role of APPL1 in the modulation of PDN in STZ-induced diabetic rats, which might be attributed to the negative regulation of mTOR activation.

APPL1 overexpression enhanced the phosphorylation of AMPK and inhibited the phosphorylation of Akt in STZ-induced diabetic rats

Ample evidence has demonstrated that AMPK and Akt are the upstream effectors of mTOR.²⁴ Thus, we subsequently investigated whether APPL1 could negatively regulate mTOR via the AMPK or Akt in STZ-induced diabetic rats. The results of Western blotting exhibited that the phosphorylation of AMPK was significantly reduced, whereas the phosphorylation of Akt was markedly elevated in PDN rats versus the control rats

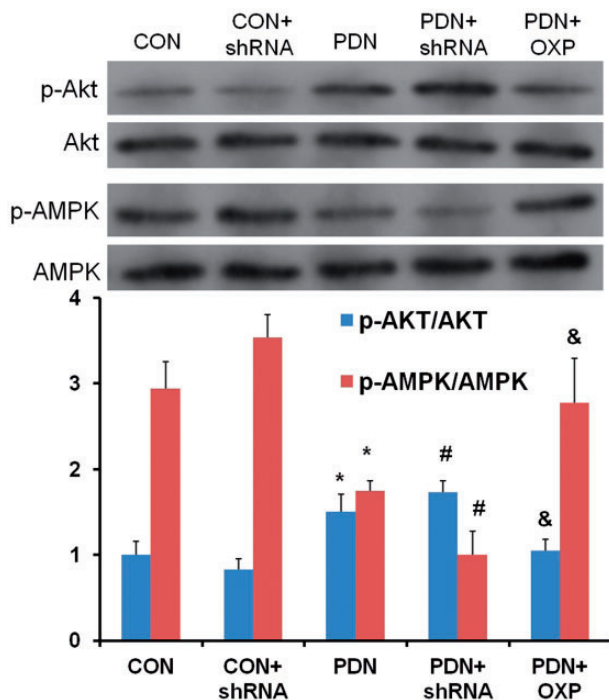


Figure 7. The involvement of AMPK and Akt in the negative regulation of mTOR by APPL1 in STZ-induced diabetic rats. The variations of p-AMPK and p-Akt in normal control rats with vacant lentiviral vector control, normal control rats with APPL1 knock-down, PDN rats, and PDN rats with APPL1 knockdown, and PDN rats with APPL1 overexpression. The abbreviations for the groups of negative control, normal control + shRNA encoding APPL1, painful diabetic neuropathy (PDN), PDN + shRNA encoding APPL1 (shRNA) and PDN + APPL1 genetic overexpression are shown as CON, CON + shRNA, PDN, PDN + shRNA, and PDN + OXP. (n = 4, * $P < 0.05$ vs. NC group, # $P < 0.05$ vs. PDN group). Data are expressed as the means \pm SEM.

($P < 0.05$; Figure 7). APPL1 deficiency evidently contributed to the inhibition of the phosphorylation of AMPK and the augmented phosphorylation of Akt in PDN rats. APPL1 overexpression rescued the phosphorylation of AMPK and inhibited the phosphorylation of Akt in PDN rats ($P < 0.05$; Figure 7). These results showed that the negative regulation of mTOR by APPL1 in the pathogenesis of PDN might be attributed to its modulation for the phosphorylation of AMPK and Akt.

Interaction of APPL1 with Rab5 and negative modulation of the Rab5 activity in the spinal cord in PDN rats

As an adaptor endosomal protein, APPL1 has been identified to be related to Rab5, with its intracellular co-localization with Rab5 in dendrites.²³ To further interrogate the relevance of APPL1 and Rab5 in the condition of PDN, the variation of Rab5 expression in STZ-induced diabetic rats was investigated for the correlation with APPL1 suppression or overexpression. Initially, the expression and localization of Rab5 were determined in both control rats and PDN rats by the immunofluorescent assay. The results documented that Rab5 was expressed in astrocytes and neurons in the control rats, authenticating its co-expression with NeuN ($56\% \pm 7.2$; Figure 8(a)) and GFAP ($89\% \pm 9.6$; Figure 8(b)), which was upregulated in PDN rats. Rab5 was mainly localized in the lamina I in spinal dorsal horn in the control rats, while its expression was significantly enhanced in the lamina I and lamina II in the spinal dorsal horn in the PDN rats, indicating the co-expression with CGRP, which was primarily in the C and A sensory fibers ($63\% \pm 5.8$; Figure 8(c)).²⁵ The alteration of Rab5 was detected with the presence or absence of APPL1 afterward. The Western blotting exhibited that Rab5 was significantly elevated in PDN rats versus the control rats, whereas KD of APPL1 expression by shRNA targeting APPL1 significantly enhanced the elevation of Rab5 versus the PDN rats ($P < 0.05$; Figure 9(a)). Consistently, the enrichment of Rab5 expression significantly subsided in the case of APPL1 overexpression ($P < 0.05$; Figure 9(b)). For further validation, immunostaining for Rab5 in lumbar spinal dorsal horn in APPL1 genetic KD or overexpression diabetic rats was employed. The results revealed that Rab5 was mainly located in the superficial layer of spinal dorsal horn in the control rats and evidently increased in PDN rats ($P < 0.05$; Figure 9(c) and (d)). In parallel, employment of shRNA targeting APPL1 significantly reduced the immunoreactivity of Rab5, whereas APPL1 overexpression pronouncedly augmented the immunoreactivity of Rab5 ($P < 0.05$; Figure 9(c) and (d)). These data demonstrated that APPL1 in effect

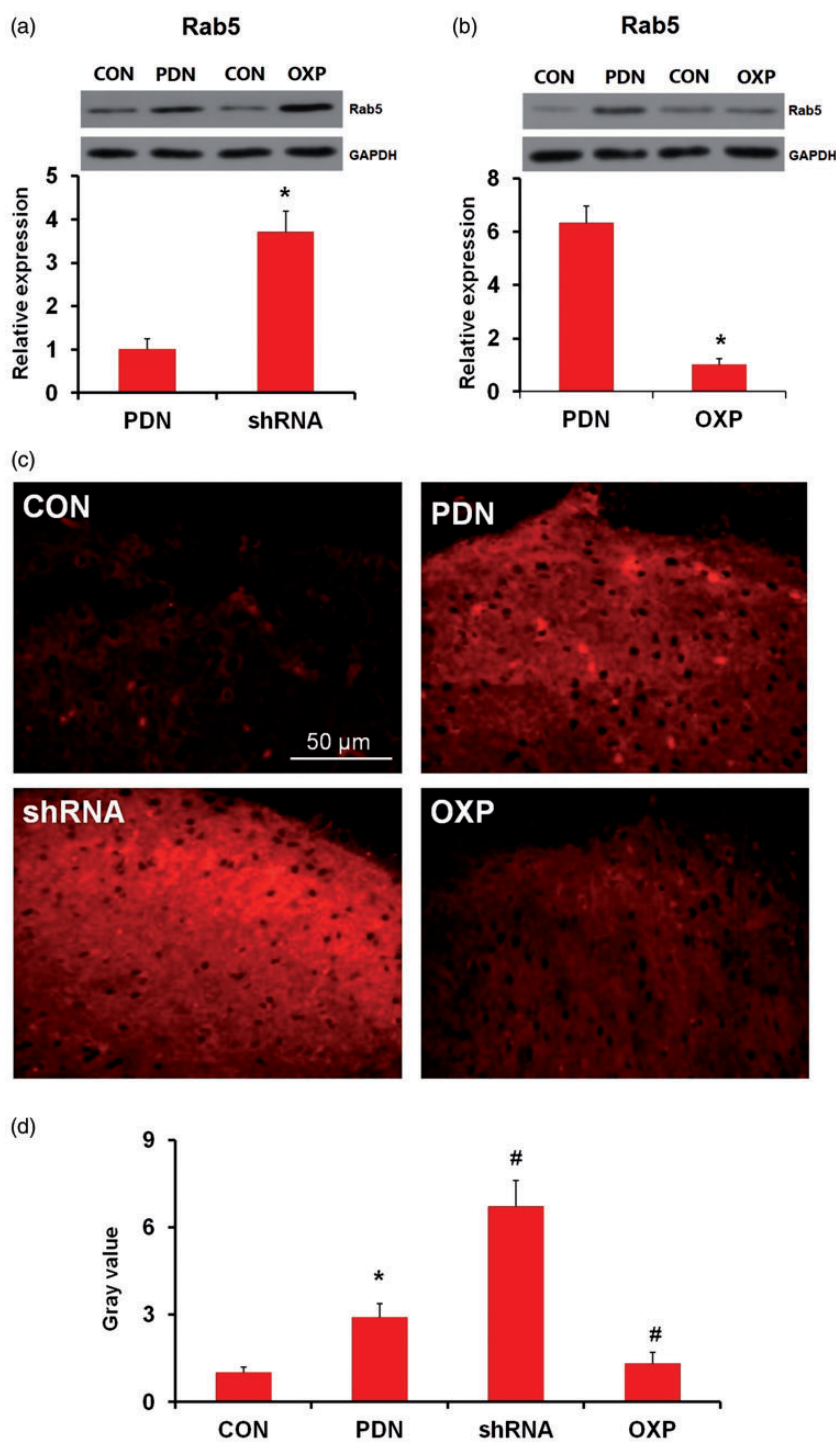


Figure 8. Effects of APPL1 genetic knockdown or overexpression on Rab5 expression in STZ-induced diabetic rats. (a) Effects of APPL1 knockdown on Rab5 expression in STZ-induced diabetic rats. (b) Effects of APPL1 genetic overexpression on Rab5 expression in STZ-induced diabetic rats. (c) to (d) Immunostaining for Rab5 in lumbar spinal dorsal horn in APPL1 genetic knockdown or overexpression diabetic rats. The upper panel shows the immunoactivity of Rab5 in lumbar spinal dorsal horn of diabetic rats; the lower bars show the levels of Rab5 by quantifying the gray value of Rab5 immunostaining images. The abbreviations for the groups of normal control, painful diabetic neuropathy (PDN), PDN + APPL1 genetic knockdown, and PDN + APPL1 genetic overexpression are shown as CON, PDN, shRNA, and OXP, respectively (n = 20 for immunofluorescent staining assay, n = 4 for Western blotting assay, * $P < 0.05$ vs. PDN group in Figure 8(a) and (b); * $P < 0.05$ vs. CON group, # $P < 0.05$ vs. PDN group in Figure 8(d)). Data are expressed as the means \pm SEM. GAPDH: glyceraldehyde 3-phosphate dehydrogenase.

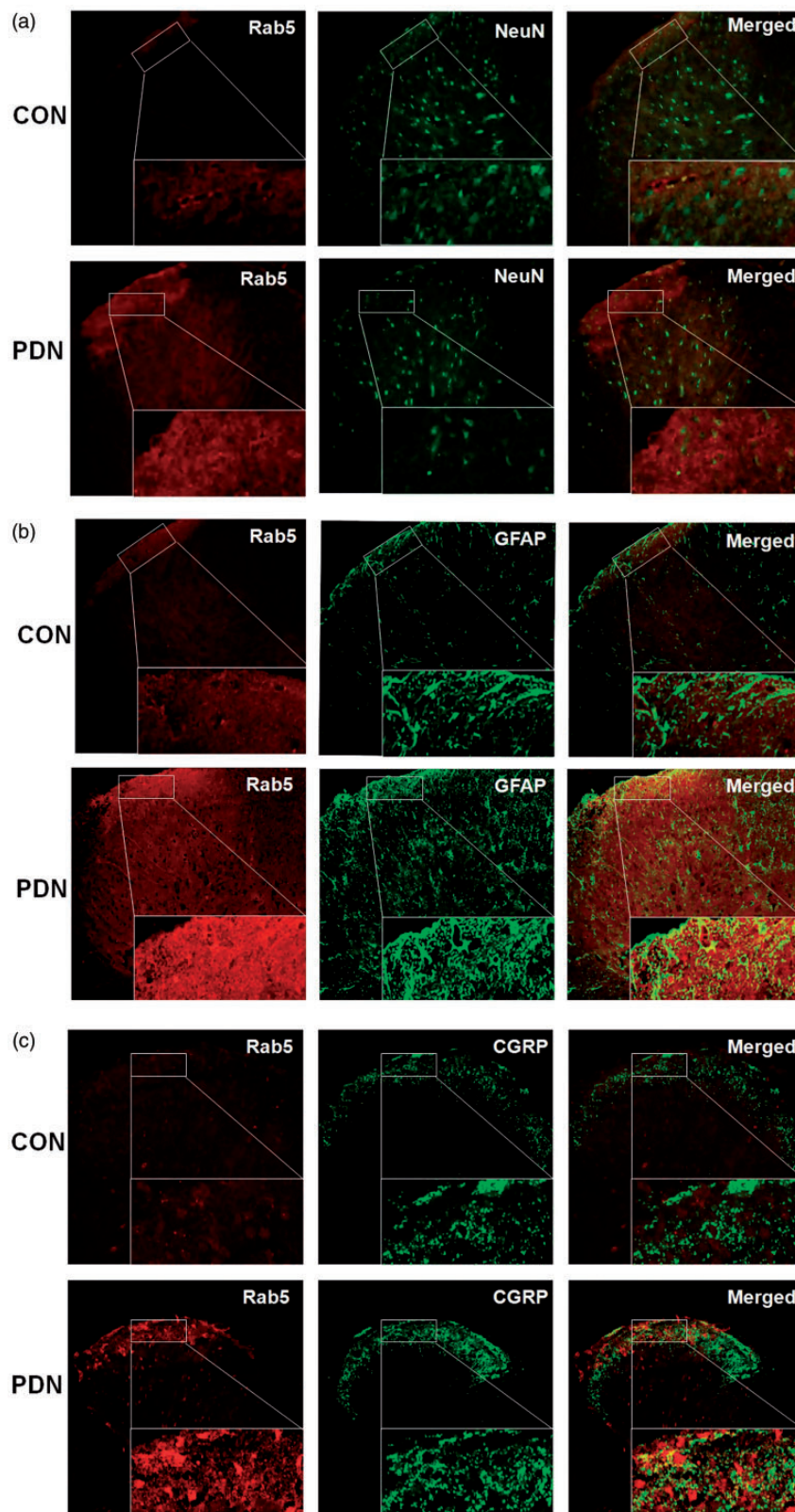


Figure 9. The localization and distribution of Rab5 in the spinal cord in STZ-induced diabetic rats. (a) to (c) Double labeling of Rab5 (red) with NeuN (green), GFAP (green), and CGRP (green) in normal control (CON) rats and PDN rats. (n = 20). PDN: painful diabetic neuropathy; CON: normal control; CGRP: calcitonin gene-related peptide; GFAP: glial fibrillary acidic protein.

interacted with Rab5 and regulated the Rab5 in a negative manner. Consistently, the enrichment of Rab5 expression significantly subsided in the case of APPL1 overexpression ($P < 0.05$; Figure 9(b)). For further validation, immunostaining was employed for Rab5 in lumbar spinal dorsal horn in diabetic rats with APPL1 overexpression or genetic KD of APPL1. The results revealed that Rab5 was mainly located in the superficial layer of spinal dorsal horn in the control rats and evidently increased in PDN rats ($P < 0.05$; Figure 9(c) and (d)). In parallel, employment of shRNA targeting APPL1 significantly reduced the immunoreactivity of Rab5, whereas APPL1 overexpression pronouncedly augmented the immunoreactivity of Rab5 ($P < 0.05$; Figure 9(c) and (d)). These data demonstrated that APPL1 *de facto* interacted with Rab5 and regulated the Rab5 in a negative manner.

Discussion

PDN is a debilitating disorder related to axonal atrophy, dull regenerative potential demyelination, and loss of peripheral nerve fibers. The complicated pathogenesis of PDN may be involved in a diversity of mechanisms, such as deficits of metabolic neurotrophic factors, microvascular injury, inflammation, and neuro-immune interactions.²⁶ Despite advances in the etiology of PDN, there are scant therapies approved for the pharmacological therapy of painful or insensate PDN. Therefore, the development of novel therapeutic strategies still remains crucial.

Our experiment had strength. We did detect a significant decrease in mechanical and a slight decrease in thermal pain threshold of PDN rats. Moreover, we found APPL1 shRNA further aggravates mechanical hyperalgesia rather than thermal hyperalgesia in diabetic rats. Because diabetic rats have severe urinary frequency and polyuria symptoms, and even if the urine of platform and the tested rat paws was timely wiped in the process of TWL detection, it would inevitably bring huge errors as the tested rat paws were frequently moistened and could resist thermal pain better. Moreover, we have found that TWL was significantly decreased at two weeks post injection when polyuria symptoms were very slight and returned to no statistical significance in three to four weeks when polyuria symptoms were significantly deteriorated in the STZ-injected rats versus the control rats (Figure 2(c)), which indicates that polyuria symptoms may affect behavioral measurement of TWL to some extent. Our research also had some limitations. Despite our results, we still could not exclude that APPL1 shRNA has any effect on thermal hypersensitivity, nor the trivia of implicated contribution of APPL1 in the development of PDN in rats herein.

APPL1, or DIP13 α , is a 709 amino acid endosomal protein that serves as a relay to interact with a range of proteins.²⁷ Notably, DM mainly results from relative insulin deficiency, which is attributed to impaired signaling or defective insulin secretion.²⁸ The main peripheral insulin targets, including skeletal muscles, adipose tissues, and the liver, where the APPL1 expression has been determined, indicate the involvement of APPL1 in DM.⁸ However, the role of APPL1 in the condition of PDN remains a puzzle. In our experiment, the protein levels of APPL1 were significantly reduced in the spinal dorsal cord in PDN rats versus the control rats, which was supported by the prior report suggesting that the APPL1 is also dramatically reduced in pancreatic β cells in diabetic mice.²⁹ The reduction of APPL1 synchronously affected mechanical and thermal pain hypersensitivity, rather than cold pain hypersensitivity, in STZ-induced diabetic rats. The localization of APPL1 was further determined in control rats and PDN rats by immunofluorescent staining assay. APPL1 was abundantly expressed in the lamina of spinal dorsal horn, which was mainly localized in spinal dorsal horn neurons and microglia, and weakly expressed in astrocytes in the control rats. The APPL1 was significantly downregulated in laminae I and II and slightly decreased in laminae III to VI in spinal dorsal horn in PDN rats as compared with control rats. APPL1 has been identified to affect the synaptic plasticity.²³ Accordingly, the effect of APPL1 on the formation of dendritic spine and synapse in the pathogenesis of PDN was probed. Indeed, APPL1 deficiency enhanced the augmentation of the formation of dendritic spine and synapse, and conversely, APPL1 enrichment gave rise to the opposite results. However, our results were conflicting to another report in which APPL1 increased the spine and synaptic density in hippocampal neurons.¹⁶ This discrepant effect of APPL1 on the development of dendritic spine and synapse might be attributed to the heterogeneity of different locations. Nevertheless, the molecular mechanism underlying the modulation of hyperalgesia by APPL1 via regulating the formation of dendritic spine and synapse remains obscure.

Recently, mTOR has garnered attention of researchers in the field of synaptic plasticity and has been proved to exert a crucial role in neuropathic pain.^{30,31} The mTOR activity in dorsal root ganglion neurons was pronouncedly increased by the sensitizing receptors and peripheral nerve injury.^{30,32} There is also potent evidence linking the augmented mTORC1 activity to the plasticity in the spinal dorsal horn subsequent to peripheral injury.^{33,34} In addition, mTOR is also considered essential to the insulin signaling pathway, and modulation of glucose uptake and glycogen synthesis.³⁵ However, the association between APPL1 and mTOR in PDN remains masked. Herein, we addressed whether APPL1 could

influence the expression of mTOR in STZ-induced diabetic rats with PDN. We employed immunofluorescent staining assay to visualize the distinct localization of APPL1 and p-mTOR in the spinal cord in both PDN rats and the control rats. The results of immunohistochemistry exhibited that APPL1 was widely expressed in both the gray matter and the white matter of the lumbar spinal cord. Specifically, the expression levels of APPL1 and p-TOR were remarkably enhanced in the superficial layer of the spinal dorsal horn, laminae I and II, which are the most extensively explored locations in the pain processing and exert a central role in the sensory information transmission.³⁶ In contrast, the faint expression of APPL1 was accompanied by monstrous expression of p-mTOR in PDN rats, suggesting that the APPL1 expression was eliminated in PDN condition and was negatively correlated with the m-TOR activation.

To further confirm the exact effect of APPL1 in PDN as well as the effect on the regulation of mTOR in STZ-induced diabetic rats, spinal APPL1 was locally knocked down by lentiviral vector system. The behavioral tests demonstrated that the MWTs in PDN rats were remarkably decreased with the treatment of APPL1 shRNA vector versus those control rats treated with saline, suggestive of the APPL1 deletion aggregating the mechanical hyperalgesia in diabetic rats. Concurrently, spinal KD of APPL1 further upregulated the levels of p-mTOR in PDN rats, suggesting that APPL1 negatively regulated the activation of mTOR. In parallel, the overexpression of APPL1 in diabetic rats dramatically increased the MWTs and TWLs in diabetic rats with PDN and significantly inhibited the expression of p-mTOR in the spinal cord in ob/ob mice. Rapamycin, the mTOR inhibitor, could mitigate the hyperalgesia in PDN rats. On the basis of our aforementioned data, APPL1 negatively modulated the activation of mTOR in the pathogenesis of PDN. Nonetheless, the molecular event that drives the modulation of mTOR by APPL1 remains elusive. APPL1 has been shown to regulate the activities of AMPK in response to stimulation from insulin or growth factor signaling.⁸ mTOR as the well-defined target of AMPK is explicitly implicated in the modulation of synaptic plasticity.^{37,38} In addition, Akt, a well-known upstream effector of mTOR, exerts a crucial role in pathogenesis of pain.³⁹ APPL1 was identified to interact with Akt and modulate the activity of Akt.¹⁵ Thus, the involvement of Akt in the condition of PDN invited the confirmation of our speculation.

We speculated that APPL1 negatively regulated mTOR in the pathogenesis of PDN probably via the modulation of AMPK and Akt. The results revealed that APPL1 activated the phosphorylation of AMPK and inhibited the phosphorylation of Akt. Of note, endosomes have emerged as paramount machinery for signal transduction from cell membrane to the nuclei.⁴⁰

The small GTPase Rab5 has been identified as a paramount regulator of transport from the plasma membrane to early endosomes, and continuous cycles of GDP/GTP exchange and hydrolysis regulate endocytosis.⁴¹ APPL1 has been reported to interact with Rab5 mediating the adiponectin signaling.⁸ In our experiment, Rab5 was abundantly expressed in astrocytes and neurons in the normal rats, with its expression significantly upregulated in the PDN rats. In addition, Rab5 was colocalized with CGRP, which exhibited a central role in the development of peripheral sensitization and related enhanced pain,²⁵ implying the involvement of Rab5 in the process of PDN. Subsequently, we affirmed that in contrast to the control rats, Rab5, which was mainly expressed in the superficial layer of spinal dorsal horn, was significantly increased in STZ-induced diabetic rats, whereas the APPL1 inhibition increased the Rab5 expression, and the APPL1 overexpression decreased the Rab5 expression, respectively. Moreover, the Rab5 activation selectively suppressed the mTOR activation.⁴² KD of Rab5 could block the insulin-evoked activation of Akt43. Thus, it is justifiable to speculate that the APPL1 deficiency may lead to Rab5 activation, thus directly or indirectly inhibiting the mTOR activity and eventually exacerbating the hyperalgesia in the condition of PDN.

APPL1 has also been authenticated to potentiate the insulin sensitivity by facilitating the binding of insulin receptor substrate proteins 1 and 2 (IRS1/2) to the insulin receptor.⁹ Furthermore, IR and pIRS-1 are mainly located in neurons in the superficial layer of the spinal dorsal horn in STZ-induced diabetic rats. The reduction of IR and pIRS-1 in the spinal dorsal horn was consistent with the progressive mechanical hyperalgesia in ob/ob mice.⁴³ Thus, the regulation of hyperalgesia by APPL1 might also be attributable to the modulation of IRS1/2 in the pathogenesis of PDN. The present experiment cannot exclude the possibility that the regulation of PDN by APPL1 was mediated via the regulation of IRS or other insulin signaling pathways.

In our study, we adopted MAP2 and Bassoon as markers for quantitative analysis of dendritic spine and synapse density, respectively.^{44,45} We showed that APPL1 was implicated in regulating the formation of dendritic spine and synapse, as APPL1 deficiency further promoted their formation in diabetic rats.

Conclusion

Collectively, despite the multifaceted functionalities of APPL1 in the pathogenesis of PDN, our data depicted that APPL1 exerted a protective effect in PDN rats and negatively regulated the activity of mTOR, probably via the modulation of Rab5/Akt or AMPK signaling

pathways, which confers the potential of APPL1 as a therapeutic target in PDN.

Author Contributions

W-YH contributed to the conception of the study and manuscript drafting as well as article revision. W-YH, JH, YW, LZ, and Q-MX conducted the experiments. W-YH, BZ, W-CZ, and H-BW were responsible for the acquisition and interpretation of the data. All authors read and approved the current version for publication.


Declaration of Conflicting Interests

The author(s) declared no potential conflicts of interest with respect to the research, authorship, and/or publication of this article.

Funding

The author(s) disclosed receipt of the following financial support for the research, authorship, and/or publication of this article: This study was supported by a grant from National Natural Science Foundation of China (no. 81771357) and Guangdong National Science Foundation (no. 2017A030313587).

ORCID iD

Han-Bing Wang  <https://orcid.org/0000-0003-0145-0081>

References

1. Yang W, Lu J, Weng J, Jia W, Ji L, Xiao J, Shan Z, Liu J, Tian H, Ji Q, Zhu D, Ge J, Lin L, Chen L, Guo X, Zhao Z, Li Q, Zhou Z, Shan G, He J. Prevalence of diabetes among men and women in China. *New Engl J Med* 2010; 362: 1090–2426.
2. Gordo A, Scuffham P, Shearer A, Oglesby A, Tobian JA. The health care costs of diabetic peripheral neuropathy in the US. *Diabetes Care* 2003; 26: 1790–1795.
3. Tesfaye S, Boulton AJM, Dyck PJ, Freeman R, Horowitz M, Kempner P, Lauria G, Malik RA, Spallone V, Vinik A, Bernardi L, Valensi P. Diabetic neuropathies: update on definitions, diagnostic criteria, estimation of severity, and treatments. *Diabetes Care* 2010; 33: 2285–2293.
4. Woolf CJ, Mannion RJ. Neuropathic pain: aetiology, symptoms, mechanisms, and management. *Lancet* 1999; 353: 1959–1964.
5. Bierhaus A, Fleming T, Stoyanov S, Leffler A, Babes A, Neacsu C, Sauer SK, Eberhardt M, Schnölzer M, Lasitschka F, Lasitschka F, Neuhuber WL, Kichko TI, Konrade I, Elvert R, Mier W, Pirags V, Lukic IK, Morcos M, Dehmer T, Rabbani N, Thornalley PJ, Edelstein D, Nau C, Forbes J, Humpert PM, Schwaninger M, Ziegler D, Stern DM, Cooper ME, Haberkorn U, Brownlee M, Reeh PW, Nawroth PP. Methylglyoxal modification of Nav1.8 facilitates nociceptive neuron firing and causes hyperalgesia in diabetic neuropathy. *Nat Med* 2012; 18: 926–933.
6. Bellows BK, Nelson RE, Oderda GM, LaFleur J. Long-term cost-effectiveness of initiating treatment for painful diabetic neuropathy with pregabalin, duloxetine, gabapentin, or desipramine. *Pain* 2016; 157: 203–213.
7. Cheng KKY, Lam KSL, Wang Y, Huang Y, Carling D, Wu D, Wong C, Xu A. Adiponectin-induced endothelial nitric oxide synthase activation and nitric oxide production are mediated by APPL1 in endothelial cells. *Diabetes* 2007; 56: 1387–1394.
8. Mao X, Kikani CK, Riojas RA, Langlais P, Wang L, Ramos FJ, Fang Q, Christ-Roberts CY, Hong JY, Kim R-Y, Liu F, Dong LQ. APPL1 binds to adiponectin receptors and mediates adiponectin signalling and function. *Nat Cell Biol* 2006; 8: 516–523.
9. Ryu J, Galan AK, Xin X, Dong F, Abdul-Ghani MA, Zhou L, Wang C, Li C, Holmes BM, Sloane LB, Austad SN, Guo S, Musi N, DeFronzo RA, Deng C, White MF, Liu F, Dong LQ. APPL1 potentiates insulin sensitivity by facilitating the binding of IRS1/2 to the insulin receptor. *Cell Rep* 2014; 7: 1227–1238.
10. Cheng KKY, Iglesias MA, Lam KSL, Wang Y, Sweeney G, Zhu W, Vanhoutte PM, Kraegen EW, Xu A. APPL1 potentiates insulin-mediated inhibition of hepatic glucose production and alleviates diabetes via Akt activation in mice. *Cell Metab* 2009; 9: 417–427.
11. Deepa SS, Dong LQ. APPL1: role in adiponectin signaling and beyond. *Am J Physiol Endocrinol Metab* 2009; 296: E22–E36.
12. Zhou L, Deepa SS, Etlzer JC, Ryu J, Mao X, Fang Q, Liu DD, Torres JM, Jia W, Lechleiter JD, Liu F, Dong LQ. Adiponectin activates AMP-activated protein kinase in muscle cells via APPL1/LKB1-dependent and phospholipase C/Ca²⁺/Ca²⁺/calmodulin-dependent protein kinase kinase-dependent pathways. *J Biol Chem* 2009; 284: 22426–22435.
13. Xin X, Zhou L, Reyes CM, Liu F, Dong LQ. APPL1 mediates adiponectin-stimulated p38 MAPK activation by scaffolding the TAK1-MKK3-p38 MAPK pathway. *Am J Physiol Endocrinol Metab* 2011; 300: E103–E110.
14. Schenck A, Goto-Silva L, Collinet C, Rhinn M, Giner A, Habermann B, Brand M, Zerial M. The endosomal protein Appl1 mediates Akt substrate specificity and cell survival in vertebrate development. *Cell* 2008; 133: 486–497.
15. Wang Y-B, Wang J-J, Wang S-H, Liu S-S, Cao J-Y, Li X-M, Qiu S, Luo J-H. Adaptor protein APPL1 couples synaptic NMDA receptor with neuronal prosurvival phosphatidylinositol 3-kinase/Akt pathway. *J Neurosci* 2012; 32: 11919–11929.
16. Majumdar D, Nebhan CA, Hu L, Anderson B, Webb DJ. An APPL1/Akt signaling complex regulates dendritic spine and synapse formation in hippocampal neurons. *Mol Cell Neurosci* 2011; 46: 633–644.
17. He W-y, Zhang B, Xiong Q-m, Yang C-x, Zhao W-c, He J, Zhou J, Wang H-B. Intrathecal administration of rapamycin inhibits the phosphorylation of DRG Nav1.8 and attenuates STZ-induced painful diabetic neuropathy in rats. *Neurosci Lett* 2016; 619: 21–28.
18. Chaplan SR, Bach FW, Pogrel JW, Chung JM, Yaksh TL. Quantitative assessment of tactile allodynia in the rat paw. *J Neurosci Meth* 1994; 53: 55–63.

19. Kim SK, Park JH, Bae SJ, Kim JH, Hwang BG, Min B-I, Park DS, Na HS. Effects of electroacupuncture on cold allodynia in a rat model of neuropathic pain: mediation by spinal adrenergic and serotonergic receptors. *Exp Neurol* 2005; 195: 430–436.
20. Hargreaves K, Dubner R, Brown F, Flores C, Joris J. A new and sensitive method for measuring thermal nociception in cutaneous hyperalgesia. *Pain* 1988; 32: 77–88.
21. Cao XC, Pappalardo LW, Waxman SG, Tan AM. Dendritic spine dysgenesis in superficial dorsal horn sensory neurons after spinal cord injury. *Mol Pain* 2017; 13: 119.
22. Mills EP, Di Pietro F, Alshelh Z, Peck CC, Murray GM, Vickers ER, Henderson LA. Brainstem pain-control circuitry connectivity in chronic neuropathic pain. *J Neurosci* 2018; 38: 465–473.
23. Fernandez-Monreal M, Sanchez-Castillo C, Esteban JA. APPL1 gates long-term potentiation through its plekstrin homology domain. *J Cell Sci* 2016; 129: 2793–2803.
24. Xu Y, Liu C, Chen S, Ye Y, Guo M, Ren Q, Liu L, Zhang H, Xu C, Zhou Q, Huang S, Chen L. Activation of AMPK and inactivation of Akt result in suppression of mTOR-mediated S6K1 and 4E-BP1 pathways leading to neuronal cell death in in vitro models of Parkinson's disease. *Cell Signal* 2014; 26: 1680–1689.
25. Iyengar S, Ossipov MH, Johnson KW. The role of calcitonin gene-related peptide in peripheral and central pain mechanisms including migraine. *Pain* 2017; 158: 543–559.
26. Callaghan BC, Cheng HT, Stables CL, Smith AL, Feldman EL. Diabetic neuropathy: clinical manifestations and current treatments. *Lancet Neurol* 2012; 11: 521–534.
27. Liu Y, Zhang C, Zhao L, Du N, Hou N, Song T, Huang C. APPL1 promotes the migration of gastric cancer cells by regulating Akt2 phosphorylation. *Int J Oncol* 2017; 51: 1343–1351.
28. Han W. Dual functions of adaptor protein, phosphotyrosine interaction, PH domain and leucine zipper containing 1 (APPL1) in insulin signaling and insulin secretion. *Proc Natl Acad Sci USA* 2012; 109: 8795–8796.
29. Cheng KKY, Lam KSL, Wu D, Wang Y, Sweeney G, Hoo RLC, Zhang J, Xu A. APPL1 potentiates insulin secretion in pancreatic beta cells by enhancing protein kinase Akt-dependent expression of SNARE proteins in mice. *Proc Natl Acad Sci USA* 2012; 109: 8919–8924.
30. Melemedjian OK, Asiedu MN, Tillu DV, Sanoja R, Yan J, Lark A, Khoutorsky A, Johnson J, Peebles KA, Lepow T, Sonenberg N, Dussor G, Price TJ. Targeting adenosine monophosphate-activated protein kinase (AMPK) in pre-clinical models reveals a potential mechanism for the treatment of neuropathic pain. *Mol Pain* 2011; 7: 70.
31. Jimenez-Diaz L. Local translation in primary afferent fibers regulates nociception. *PLoS One* 2008; 3: e1961.
32. Melemedjian OK, Asiedu MN, Tillu DV, Peebles KA, Yan J, Ertz N, Dussor GO, Price TJ. IL-6- and NGF-induced rapid control of protein synthesis and nociceptive plasticity via convergent signaling to the eIF4F complex. *J Neurosci* 2010; 30: 15113–15123.
33. Asante CO, Wallace VC, Dickenson AH. Formalin-induced behavioural hypersensitivity and neuronal hyperexcitability are mediated by rapid protein synthesis at the spinal level. *Mol Pain* 2009; 5: 27.
34. Asante CO, Wallace VC, Dickenson AH. Mammalian target of rapamycin signaling in the spinal cord is required for neuronal plasticity and behavioral hypersensitivity associated with neuropathy in the rat. *J Pain* 2010; 11: 1356–1367.
35. Saltiel AR, Kahn CR. Insulin signalling and the regulation of glucose and lipid metabolism. *Nature* 2001; 414: 799–806.
36. Todd AJ. Neuronal circuitry for pain processing in the dorsal horn. *Nat Rev Neurosci* 2010; 11: 823–836.
37. Price TJ, Das V, Dussor G. Adenosine monophosphate-activated protein kinase (AMPK) activators for the prevention, treatment and potential reversal of pathological pain. *Curr Drug Targets* 2016; 17: 908–920.
38. Ling Y-Z, Li Z-Y, Ou-Yang H-D, Ma C, Wu S-L, Wei J-Y, Ding H-H, Zhang X-L, Liu M, Liu C-C, Huang Z-Z, Xin W-J. The inhibition of spinal synaptic plasticity mediated by activation of AMP-activated protein kinase signaling alleviates the acute pain induced by oxaliplatin. *Exp Neurol* 2017; 288: 85–93.
39. Guo JR, et al. Effect and mechanism of inhibition of PI3K/Akt/mTOR signal pathway on chronic neuropathic pain and spinal microglia in a rat model of chronic constriction injury. *Oncotarget* 2017; 8: 52923–52934.
40. Miaczynska M, Christoforidis S, Giner A, Shevchenko A, Uttenweiler-Joseph S, Habermann B, Wilm M, Parton RG, Zerial M. APPL proteins link Rab5 to nuclear signal transduction via an endosomal compartment. *Cell* 2004; 116: 445–456.
41. Rybin V, Ullrich O, Rubino M, Alexandrov K, Simon I, Seabra MC, Goody R, Zerial M. GTPase activity of Rab5 acts as a timer for endocytic membrane fusion. *Nature* 1996; 383: 266–269.
42. Li L, Kim E, Yuan H, Inoki K, Goraksha-Hicks P, Schiesher RL, Neufeld TP, Guan K-L. Regulation of mTORC1 by the Rab and Arf GTPases. *J Biol Chem* 2010; 285: 19705–19709.
43. Kou Z-Z, Li C-Y, Tang J, Hu J-C, Qu J, Liao Y-H, Wu S-X, Li H, Li Y-Q. Down-regulation of insulin signaling is involved in painful diabetic neuropathy in type 2 diabetes. *Pain Physician* 2013; 16: E71–E83.
44. Caceres A, Banker G, Steward O, Binder L, Payne M. MAP2 is localized to the dendrites of hippocampal neurons which develop in culture. *Brain Res* 1984; 315: 314–318.
45. Dick O, Tom Dieck S, Altmann WD, Ammermüller J, Weiler R, Garner CC, Gundelfinger ED, Brandstätter JH. The presynaptic active zone protein bassoon is essential for photoreceptor ribbon synapse formation in the retina. *Neuron* 2003; 37: 775–786.